PROCEEDINGS OF SCIENCE

PoS(NIC XI)194

Measurement of the ^{24,25,26}Mg(n,γ) reaction cross-section at n_TOF

C. Massimi*[1], S. Andriamonje[2], J. Andrzejewski[3], L. Audouin[4], V. Bécares[5], F. Bečvář[6], F. Belloni[7], B. Berthier[4], E. Berthoumieux[8], M. Brugger[2], M. Calviani[2], F. Calviño[9], D. Cano-Ott[5], C. Carrapiço[10], F. Cerutti[2], E. Chiaveri[2], M. Chin[2], N. Colonna[11], G. Cortés[9], M.A. Cortés-Giraldo[12], I. Dillmann[13], C. Domingo-Pardo[14], I. Duran[15], M. Fernández-Ordóñez[5], A. Ferrari[2], K. Fraval[8], S. Ganesan[16], G. Giubrone[17], M.B. Gómez-Hornillos[9], I.F. Gonçalves[10], E. González-Romero[5], F. Gramegna[18], C. Guerrero[5], F. Gunsing[8], S. Harrisopulos[19], M. Heil[14], K. Ioannides[20], E. Jericha[21], Y. Kadi[2], F. Käppeler[22], D. Karadimos[20], M. Krtička[6], E. Lebbos[2], C. Lederer[23], H. Leeb[21], R. Losito[2], M. Lozano[12], J. Marganiec[3], S. Marrone[11], T. Martinez[5], P.F. Mastinu[18], M. Meaze[11], E. Mendoza[5], A. Mengoni[24], P.M. Milazzo[7], C. Paradela[15], A. Pavlik[23], J. Perkowski[3], R. Plag[14], J. Praena[12], J.M. Quesada[12], T. Rauscher[25], R. Reifarth[14], F. Roman[2,26], C. Rubbia[2,27], R. Sarmento[10], G. Tagliente[11], J.L. Tain[17], D. Tarrío[15], L. Tassan-Got[4], L. Tlustos[2], G. Vannini[1], V. Variale[11], P. Vaz[10], A. Ventura[24], V. Vlachoudis[2], R. Vlastou[28], A. Wallner[23], C. Weiß[21]

PROCEEDINGS OF SCIENCE

1) Dipartimento di Fisica, Università di Bologna, and Sezione INFN di Bologna, Italy
2) European Organization for Nuclear Research (CERN), Geneva, Switzerland
3) Uniwersytet Łódzki, Lodz, Poland
4) Centre National de la Recherche Scientifique/IN2P3 - IPN, Orsay, France
5) Centro de Investigaciones Energeticas Medioambientales y Technologicas (CIEMAT), Madrid, Spain
6) Charles University, Prague, Czech Republic
7) Istituto Nazionale di Fisica Nucleare, Trieste, Italy
8) Commissariat à l'Énergie Atomique (CEA) Saclay - Irfu, Gif-sur-Yvette, France
9) Universitat Politecnica de Catalunya, Barcelona, Spain
10) Instituto Tecnológico e Nuclear (ITN), Lisbon, Portugal
11) Istituto Nazionale di Fisica Nucleare, Bari, Italy
12) Universidad de Sevilla, Spain
13) Physik Department E12 and Excellence Cluster Universe, Technische Universität München, Garching, Germany
14) GSI Helmholtzzentrum für Schwerionenforschung GmbH, Darmstadt, Germany
15) Universidade de Santiago de Compostela, Spain
16) Bhabha Atomic Research Centre (BARC), Mumbai, India
17) Instituto de Física Corpuscular, CSIC-Universidad de Valencia, Spain
18) Istituto Nazionale di Fisica Nucleare, Laboratori Nazionali di Legnaro, Italy
19) National Centre of Scientific Research (NCSR), Demokritos, Greece
20) University of Ioannina, Greece
21) Atominstitut, Technische Universität Wien, Austria
22) Karlsruhe Institute of Technology, Campus Nord, Institut für Kernphysik, Karlsruhe, Germany
23) Fakultät für Physik, Universität Wien, Austria
24) Agenzia nazionale per le nuove tecnologie, l'energia e lo sviluppo economico sostenibile (ENEA), Bologna, Italy
25) Department of Physics and Astronomy - University of Basel, Basel, Switzerland
26) Horia Hulubei National Institute of Physics and Nuclear Engineering - IFIN HH, Bucharest - Magurele, Romania
27) Laboratori Nazionali del Gran Sasso dell'INFN, Assergi (AQ),Italy
28) National Technical University of Athens (NTUA), Greece
E-mail: massimi@bo.infn.it

We have measured the neutron-induced capture cross-section of the important *s*-process isotopes of magnesium. The measurement has been performed at the neutron time-of-flight facility n_TOF at CERN. From a preliminary analysis of this new set of capture data we find that our results seem to be significantly lower than previous data and evaluations. We have also investigated the contribution of the direct capture component to the Maxwellian-averaged capture cross section.

11th Symposium on Nuclei in the Cosmos, NIC XI
July 19-23, 2010
Heidelberg, Germany

*Speaker.

PoS(NIC XI)194

1. Introduction and physical motivations

The slow neutron-capture process (*s*-process) [1, 2] in stars is responsible for the origin of about half of the elemental abundances beyond iron that we observe today. Most of the *s*-process isotopes between iron and strontium ($60 < A < 90$) are produced in massive stars ($M > 8M_{\rm sun}$) where the ^{22}Ne$(\alpha,n)^{25}$Mg reaction is the main neutron source.

Beyond strontium, the *s*-process abundances from Zr to Biare essentially produced in low mass Asymptotic Giant Branch (AGB) stars in the mass range $1.2M_{\rm sun} < M < 3M_{\rm sun}$, where most of the neutrons are provided by the ^{13}C$(\alpha,n)^{16}$O reaction and to minor part by the partial activation of the ^{22}Ne$(\alpha,n)^{25}$Mg reaction.

While ^{56}Fe represents the basic *s*-process seed for the production of the heavier isotopes, ^{25}Mg acts as an important neutron poison and affects, therefore, the neutron balance of the *s* process. Accordingly, the ^{25}Mg$(n,\gamma)^{26}$Mg cross section is required with good accuracy for a quantitative treatment of *s*-process nucleosynthesis.

1.1 Status of Mg data libraries

Existing evaluations of the Mg cross sections are presently based on the JENDL3.3 library [3]. In this evaluation the resonance parameters in the resolved resonance region were adopted from the compilation of Mughabghab [4], and negative resonances were added to reproduce the recommended thermal cross sections in Ref. [4]. The recommended thermal values are close to the experimental results of Walkiewicz *et. al* [5], but do not consider recent data of Koehler [6]. In this work previous measurements [8, 9] were reconsidered in a combined R-matrix analysis, by which the spin of several levels could be determined. Moreover, it was shown in Ref. [6] that complementary information from Ref. [10] is important for obtaining parity assignments of the nuclear levels populated in neutron reactions on ^{25}Mg+n.

Because the differences between JENDL3.3 and Ref. [6] cannot be explained by the different spin assignments for the most relevant resonances alone, a new capture measurement was performed in order to obtain improved information for an update of the (n,γ) cross sections of ^{24,25,26}Mg.

2. The experiment at CERN n_TOF

The neutron time-of-flight facility n_TOF at CERN provides a white, pulsed neutron spectrum. The description given here refers to status during phase I of the facility (2001 - 2004) when the present data were taken (for a discussion of recent improvements see Ref. [7]). Neutrons were produced by spallation of protons with 20-GeV/c from the CERN proton synchrotron in a massive ($80 \times 80 \times 60$ cm^3) lead block surrounded by 5.8 cm of cooling water, which acted also as a neutron moderator. The energy dependence of the neutron spectrum showed a $1/E$ isolethargic behavior over the energy range of interest, i.e. between 1 eV and 1 MeV. The proton pulses are characterized by a high intensity of 7×10^{12} protons per bunch and a short pulse width of 6 ns FWHM, resulting in a high-resolution, high-intensity neutron beam.

The evacuated neutron flight path to the experimental area at about 185 m from the spallation target is equipped with two collimators for reducing the beam from the initial diameter of 80 cm

to 1.8 cm at the sample position. The background in the experimental area is strongly reduced by a sweeping magnet and massive Fe and concrete walls along the flight path (for details see Refs. [11, 12]). The time between proton pulses is at least 2.4 s, long enough to prevent neutron overlap between consecutive bunches.

An array of two C_6D_6 liquid scintillators has been used as in the capture experiment. The detectors are placed perpendicular to the beam direction but shifted 9 cm upstream of the beam for reducing the effect of in-beam γ rays. Because the capture cross sections of the Mg isotopes are orders of magnitude smaller than the elastic scattering cross section, we preferred the total energy detection method [13] in combination with the Pulse Height Weighting Technique (PHWT), because of the small capture detector to be used (volume $\approx$ one liter). Background due to sample-scattered neutrons in the detector was strongly reduced by means of in-house developed C_6D_6 detectors based on a low mass carbon fiber design [14].

The neutron flux at the sample position at 185 m, which is required for determining the capture cross-section, has been measured with a well calibrated ^{235}U loaded parallel plate ionization chamber from Physikalisch-Technische Bundesanstalt at Braunschweig [15]. During the actual runs, the flux was measured and with a ^{6}Li neutron monitor [16].

The characteristics of the samples, which were disks 22 mm in diameter, are listed in Table 1. The enriched ^{25}Mg and ^{26}Mg samples consisted of magnesium-oxyde powder and were sealed in a very thin aluminum canning with a total mass of only 350 mg. The specified impurities of the enriched samples included traces of Be, Sb, Fe, Al, Sn, Mn, Cu, Ca, Mo, Ni, Ag, and Pb.

Sample	Isotopic abundance (%)			Total	Thickness		Chemical
ID	^{24}Mg	^{25}Mg	^{26}Mg	mass (g)	(cm)	(Atoms/barn[a])	form
^{nat}Mg	78.7	10.13	11.17	5.2393	0.7930	0.03415	metal
^{25}Mg	3.05	95.750	1.20	3.1924	0.2294	0.01234	oxyde
^{26}Mg	2.46	1.28	96.26	3.2301	0.2266	0.01219	oxyde

[a]Areal density of the most abundant isotope.

Table 1: Sample characteristics.

3. Data analysis

The light output of the C_6D_6 detectors is calibrated by means of mono-energetic γ-ray sources (^{137}Cs, ^{60}C0, Pu/C). The dead time of the detector is determined from the time-difference distribution of consecutive signals in each detector. From this distribution a 20-ns dead time was obtained for the actual capture setup. To avoid dead time fluctuations, a fixed value of 30 ns was considered off-line for the digitized data. The corresponding dead time correction is lower than 1% up to 750 keV neutron energy.

The determination of the capture yield (that is the probability of a capture reaction) relies on the PHWT. This technique requires a mathematical manipulation of the response function of the detection system [13], the so-called weighting function (WF). The WF is calculated by means of Monte Carlo simulations by considering the geometry and the particular design of the experimental

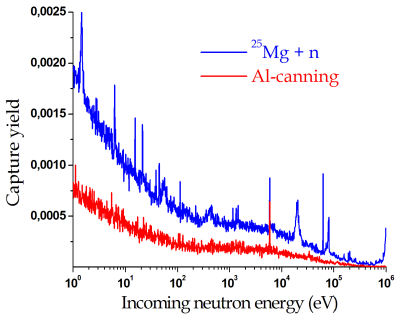

Figure 1: The ^{25}Mg(n,γ) yield together with the background contribution from the aluminum canning.

setup used. The capture yield $Y = N\frac{C_W - B}{\varphi}$ is obtained as a function of TOF from C_W, the number of weighted counts (counts multiplied by their weighting factors), corrected for the background B, and the neutron fluence φ. The fact that the sample is smaller than the neutron beam is considered by the normalization factor N. This normalization was determined with the saturated resonance method using the 4.9-eV resonance in gold [17]. The capture yield of ^{25}Mg, which represents the main result of this experiment, is plotted in Fig. 1 together with the background contribution.

The calculated capture yield is related to the capture cross-section σ_γ by the expression $Y = (1-\exp(-n\sigma_{tot})) \times \frac{\sigma_\gamma}{\sigma_{tot}}$, where n is the target thickness and σ_{tot} the total cross-section. The capture yield was analyzed with the R-matrix code SAMMY [18] for determining the resonance parameters. Experimental effects, that is multiple neutron scattering in the sample, neutron self-shielding, and experimental resolution, are properly taken into account within the SAMMY code. Preliminary resonance analyses have revealed discrepancies compared to previous evaluations. An example obtained by the simultaneous analysis of capture data from the present measurement and of transmission data from Ref. [9] is given in Fig. 2. Because the resonance shown in Fig. 2 contributes about 30% to the MACS at 30 keV, the final MACS is expected to be smaller than reported so far [6].

In addition to the resonant component, the contribution from the direct radiative capture (DRC) mechanism has been calculated. For all three isotopes, the most important (electric dipole) transitions are due to incident p-wave neutrons captured into bound levels with strong single-particle component in the *sd* shell. The resulting cross section for DRC is sensitive in this particular case to the strength of the neutron-nucleus mean field (optical) potential. Using "standard" parameters, a contribution to the MACS at kT=30 keV of less than 1 mb for each of the Mg isotope has been found. However, the presence of the single-particle 2p state close to the neutron emission threshold complicates the standard treatment of the DRC calculation in this case. Therefore, the issue still needs to be investigated in order to conclude if the DRC mechanism has a significant impact on the MACSs of the Mg isotopes.

4. Conclusions

With the present (n,γ) measurement the cross-section data on stable Mg isotopes can be im-

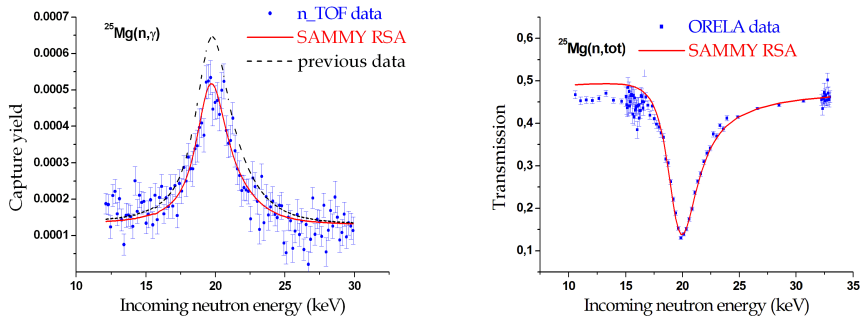

Figure 2: Simultaneous resonance shape analyses on capture and transmission data for the first s-wave resonance in the ^{25}Mg(n,γ) cross section.

proved. From preliminary analyses we find that the MACS of ^{25}Mg is lower than previously reported. The expected changes of the stellar (n,γ) rates for the Mg isotopes will have a significant impact on the neutron balance of the $s-$process.

References

[1] G Wallerstein *et al.*, Rev. Mod. Phys. **69**, 995 (1997).

[2] E. M. Burbidge, G. R. Burbidge, W. A. Fowler, and F. Hoyle, Rev. Mod. Phys. **29**, 547 (1957).

[3] K. Shibata *et. al*, J. Nucl. Sci. Technol. **39**, 1125 (2002).

[4] S. F. Mughabghab and D. I. Garber, *Neutron cross sections*, volume 1, (1984).

[5] T. A. Walkiewicz, S. Raman, E. .T. Jurney, J. W. Starner and J. E. Lynn, Phys. Rev. C **45**, 1597-1608 (1992).

[6] P. E. Koehler, Phys. Rev. C **66**, 055805 (2002).

[7] E. Chiaveri for the n_TOF Collaboration, *Int. Conf. on Nuclear Data for Science and Technology*, ND2010 (in preparation).

[8] U. N. Singh, H. I. Liou, J. Rainwater, G. Hacken and J. B. Garg, Phys. Rev. C **10**, 2150-2152 (1974).

[9] H. Weigmann, R. L. Macklin and J. A. Harvey, Phys. Rev. C **14**, 1328-1335 (1976).

[10] B. L. Berman, R. L. Van Hemert and C. D. Bowman, Phys. Rev. Lett **23**, 386-389 (1969).

[11] U. Abbondanno *et al.*, *CERN n_TOF facility: Performance report*, CERN-SL-2002-053 ECT (2003).

[12] F. Gunsing *et al.* (The n_TOF Collaboration), Nucl. Instrum. and Methods B **261**, 925-929 (2007).

[13] A. Borella, G. Aerts, F. Gunsing, M. Moxon, P. Schillebeeckx and R. Wynants, Nucl. Instrum. and Methods A **577**, 626-640 (2007).

[14] R. Plag *et al.*, Nucl. Instrum. and Methods A **496** 425-436 (2003).

[15] C. Borcea *et al.*, Nucl. Instrum. and Methods A **513**, 524-537, (2003).

[16] S. Marrone *et al.*, Nucl. Instrum. and Methods A **517**, 389-398, (2003).

[17] R. L. Macklin, J. Halperin and R. R. Winters, Nucl. Instrum. and Methods **164**, 213-214 (1979).

[18] N. M. Larson, Oak Ridge National Laboratory Report No. ORNL/TM-9179/R7.